

SIMULATION OF ICRF PLASMA HEATING IN THE VASIMR EXPERIMENT

Andrew V. Ilin^{*}, Franklin R. Chang Díaz[†], Jared P. Squire[‡], Alfonso G. Tarditi[‡],
Advanced Space Propulsion Laboratory, JSC / NASA, Houston, TX,
and Mark D. Carter[§], Oak Ridge National Laboratory, Oak Ridge, TN

ABSTRACT

Recent experiments at Advanced Space Propulsion Laboratory of the NASA Johnson Space Center, demonstrated significant ion heating at the Ion Cyclotron Range of Frequencies in the Variable Specific Impulse Magnetoplasma Rocket device. This

successful experimental work has been supported by RF-plasma interaction simulations conducted with the EMIR code. This paper reports on the implementation of an updated model for the EMIR code, from the original collisional cold plasma model, that is based on a reduced order kinetic description suitable for parallel wave propagation.

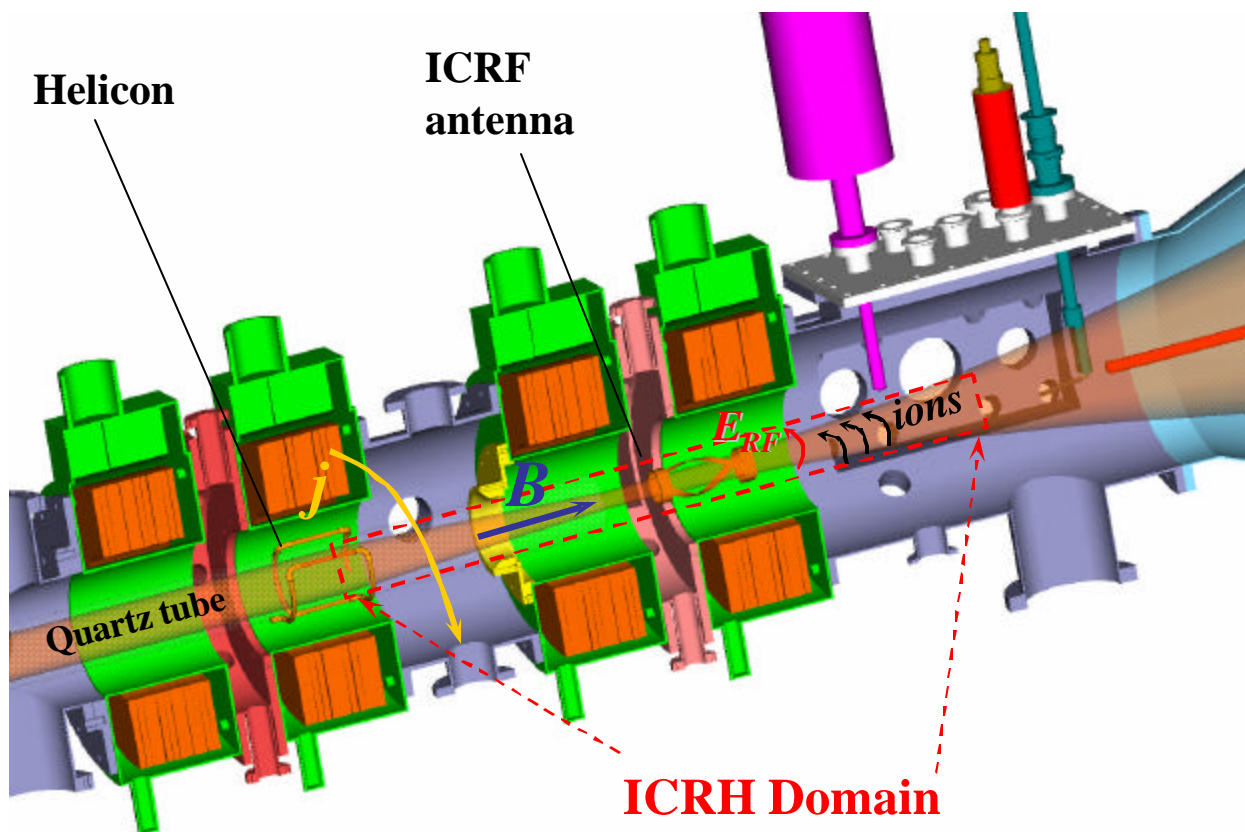


Figure 1. Ion Cyclotron Resonance Heating section in VASIMR.

^{*} AIAA member, Senior Research Scientist, Muniz Engineering, Inc., ilin@jsc.nasa.gov

[†] AIAA member, NASA Astronaut, ASPL Director

[‡] AIAA member, Senior Research Scientist, Muniz Engineering, Inc.

[§] AIAA member, Research Staff, Fusion Energy Division

MATHEMATICAL MODEL FOR RF-PLASMA INTERACTION

An important aspect of the Variable Specific Impulse Magnetoplasma Rocket (VASIMR)¹ concept is plasma heating by electromagnetic waves at the Ion Cyclotron Range of Frequencies (ICRF)². Computer simulation helps in designing an ICRF antenna for maximum absorption of RF power into the plasma in the resonance area (Figure 1).

In the EMIR code³, the RF electric field, \mathbf{E} , magnetic field, \mathbf{B} , and RF antenna current density, \mathbf{j} , are expanded in a periodic Fourier sum along the azimuthal coordinate \mathbf{f} . Harmonic dependence with respect to time t is assumed as well as azimuthal symmetry of the equilibrium quantities, so that the fields and currents in cylindrical coordinates (r, \mathbf{f}, z) can be expanded into azimuthal modes:

$$\mathbf{E}(r, \mathbf{f}, z, t) = \sum_m \mathbf{E}_m(r, z) e^{im\mathbf{f} - i\omega t}, \quad (1)$$

where m is an azimuthal mode number and ω is RF frequency.

The RF fields are obtained by solving Maxwell's equations, written in harmonic form:

$$\nabla \times \left(\frac{\mathbf{B}}{\mu} \right) = -i\omega \epsilon \mathbf{E} + \mathbf{j}_p + \mathbf{j}_{ANT}, \quad (2)$$

$$\nabla \times \mathbf{E} = i\omega \mathbf{B}, \quad (3)$$

where μ is permeability, ϵ is permittivity, \mathbf{j}_p and \mathbf{j}_{ANT} are current densities in plasma and RF antenna. Substitution of the \mathbf{B} from (3) into the (2) leads to the following wave equation for \mathbf{E} :

$$-\nabla \times \nabla \times \mathbf{E} + \frac{\omega^2}{c^2} \left(\mathbf{E} + \frac{i\mathbf{j}_p}{\omega \epsilon} \right) = -i\omega \mu \mathbf{j}_{ANT}, \quad (4)$$

where c is speed of light.

The plasma current density \mathbf{j}_p is related to the electric field by a collisional cold plasma conductivity tensor $\hat{\mathbf{S}}$: $\mathbf{j}_p = \hat{\mathbf{S}} \cdot \mathbf{E}$. Equation (4) can then be represented by a system of independent equations for \mathbf{E}_m as suggested by Stix⁴:

$$-e^{-im\mathbf{f}} \nabla \times \nabla \times \mathbf{E}_m e^{im\mathbf{f}} + \frac{\omega^2}{c^2} \hat{\mathbf{K}} \cdot \mathbf{E}_m = -i\omega \mu \mathbf{j}_m, \quad (5)$$

where $\hat{\mathbf{K}} = \mathbf{I} + \frac{i}{\omega \epsilon} \hat{\mathbf{S}}$ is a plasma dielectric tensor:

$$\hat{\mathbf{K}} = \begin{pmatrix} K_{\perp} & -iK_f & 0 \\ iK_f & K_{\perp} & 0 \\ 0 & 0 & K_{\parallel} \end{pmatrix},$$

written in the system of coordinates $(\hat{\mathbf{r}}, \hat{\mathbf{f}}, \hat{\mathbf{z}})$, $\hat{\mathbf{r}}$ and $\hat{\mathbf{z}}$ denoting, respectively, the direction perpendicular and parallel to the vacuum magnetic field \mathbf{B}_0 in the (r, z) plane, and \mathbf{j}_m is the m -th mode of the current density applied by an antenna, having only azimuthal non-zero component⁴.

In the vacuum, the electric field satisfies $\nabla \cdot \mathbf{E} = 0$, therefore Equation (5) can be simplified as

$$-e^{im\mathbf{f}} \nabla \cdot \mathbf{E}_m e^{im\mathbf{f}} + \left(\frac{\omega^2}{c^2} \right) \hat{\mathbf{K}} \cdot \mathbf{E}_m = -i\omega \mu \mathbf{j}_m. \quad (6)$$

The plasma dielectric tensor $\hat{\mathbf{K}}$ is chosen from two options: either a collisional cold plasma ($\hat{\mathbf{K}}^c$), or a reduced order kinetic description ($\hat{\mathbf{K}}^r$) suitable for parallel wave propagation.

In the cold plasma model, the entries of the dielectric tensor depend on the plasma density n_i , on the vacuum magnetic field B_0 and on the driving frequency ω as follows:

$$K_{\perp}^c = 1 - \sum_{l=e,i} \frac{\omega_{pl}^2}{\omega^2 - \omega_{cl}^2}, \quad K_f^c = \sum_{l=e,i} \frac{\omega_{ci}}{\omega} \frac{\omega_{pl}^2}{\omega^2 - \omega_{ci}^2},$$

$$K_{\parallel}^c = 1 - \sum_{l=e,i} \frac{\omega_{pl}^2}{\omega^2}, \quad \omega_{pl}^2 = \frac{q_l^2 n_l}{\epsilon m_l}, \quad \omega_{cl} = \frac{q_l B_0}{m_l},$$

where the sum is extended over the electrons and all ion species. In these equations, l denotes the electron and ion plasma species; q_l , m_l and n_l denote the species charge, mass and density. In this case the dielectric tensor does not depend on ion temperature and on flow velocity, and the wave absorption is modeled by adding an imaginary collision frequency to the RF driving frequency, which is equivalent to adding an imaginary particle mass in the dielectric

tensor elements as $m_l = \tilde{m}_l \left(1 + i \frac{n_l}{\omega} \right)$, where \tilde{m}_l is

actual real mass and n_l is effective collision frequency.

In the recent upgrade of the EMIR code, a warm plasma model was introduced in which the kinetic dispersion relation for parallel propagation⁴

$$k_{\parallel}^2 c^2 = \mathbf{w}^2 + \sum_{l=e,i} \mathbf{w}_{pl}^2 \mathbf{w} A_l^{\pm l}(k_{\parallel}) \quad (7)$$

is solved for the wave number k_{\parallel} by considering the effect of the plasma flow velocity V and the electron and ion temperature T on the conductivity. Parallel propagation can be considered using the same form for the dielectric tensor, as that used in the cold plasma model if nonlocal effects caused by perpendicular propagation can be neglected⁴. This model allows also considers the Doppler shift for the case of collisionless plasma. A reduced order formulation⁵ is used for deriving the dielectric tensor components as follows

$$\begin{aligned} K_{\perp}^r &= I + \sum_{l=e,i} \frac{\mathbf{w}_{pl}^2}{2\mathbf{w}} (A_l^{-l}(k_{\parallel}) + A_l^{+l}(k_{\parallel})), \\ K_f^r &= \sum_{l=e,i} \frac{\mathbf{w}_{pl}^2}{2\mathbf{w}} (A_l^{-l}(k_{\parallel}) - A_l^{+l}(k_{\parallel})), \\ K_{\parallel}^r &= I + \sum_{l=e,i} \frac{2\mathbf{w}_{pl}^2}{k_{\parallel} \mathbf{w}_{\perp l}^2} \left(\frac{V_l}{\mathbf{w}} + B_l^0(k_{\parallel}) \right), \end{aligned} \quad (8)$$

where k_{\parallel} is the slow wave root from Equation (7). The $A_l^{\pm l}(k_{\parallel})$ and $B_l^0(k_{\parallel})$ functions in Equation (7) and Equations (8) are given by

$$\begin{aligned} A_l^n(k_{\parallel}) &= \frac{T_{\perp l} - T_{\parallel l}}{\mathbf{w} T_{\parallel l}} + \\ &\left(\frac{V_l^n(k_{\parallel}) T_{\perp l}}{\mathbf{w} T_{\parallel l}} + \frac{n_l \mathbf{w}_{cl}}{\mathbf{w} k_{\parallel} \mathbf{w}_{\parallel l} T_{\parallel l}} \right) Z_0(V_l^n(k_{\parallel})), \\ B_l^0(k_{\parallel}) &= \frac{\mathbf{w} T_{\perp l} - k_{\parallel} V_l T_{\parallel l}}{\mathbf{w} k_{\parallel} T_{\parallel l}} + \\ &\frac{V_l^0(k_{\parallel}) T_{\perp l}}{k_{\parallel} T_{\parallel l}} Z_0(V_l^0(k_{\parallel})), \\ V_l^n(k_{\parallel}) &= \frac{\mathbf{w} - k_{\parallel} V_l - n_l \mathbf{w}_{cl}}{k_{\parallel} \mathbf{w}_{\parallel l}}, \end{aligned} \quad (9)$$

where $w_{\perp l} = \sqrt{2kT_{\perp l}/m_l}$ and $w_{\parallel l} = \sqrt{2kT_{\parallel l}/m_l}$ are the perpendicular and parallel thermal speeds of species l , T_{\perp} , T_{\parallel} are the perpendicular and parallel temperatures, k is Boltzman's constant, $n = \pm l$, and

$$Z_0(V) = \begin{cases} Z(V); k_{\parallel} > 0 \\ -Z(-V); k_{\parallel} < 0 \end{cases} \quad (10)$$

$$Z(V) = 2i \exp(-V^2) \int_{-\infty}^{iV} \exp(-t^2) dt,$$

where $Z(\mathbf{z})$ is the plasma dispersion function.

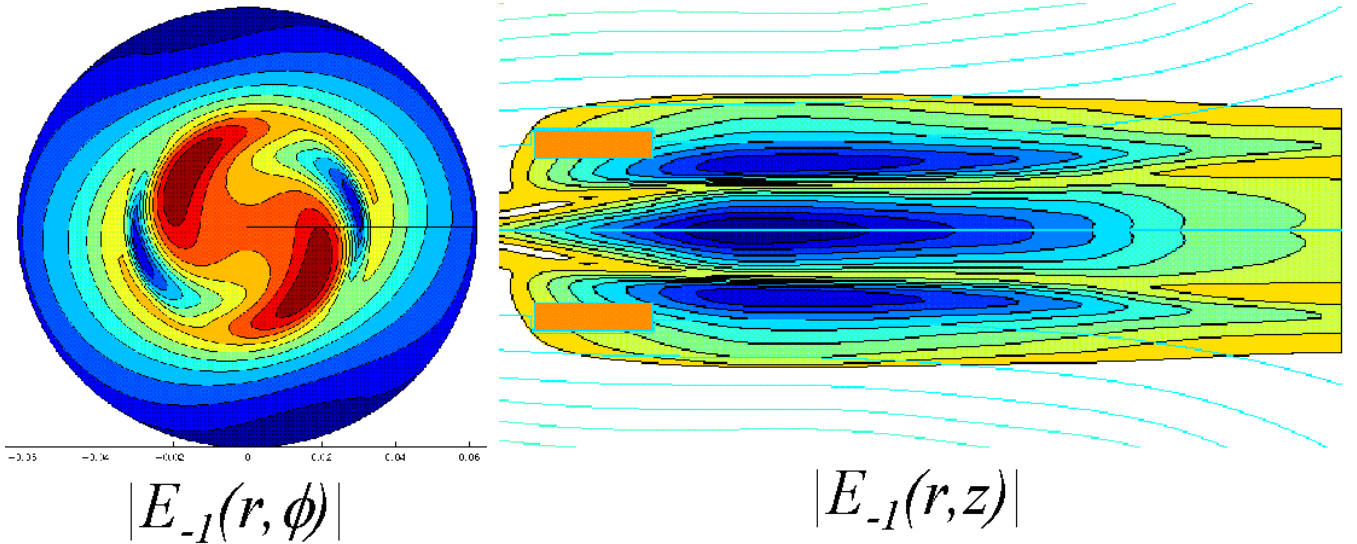


Figure 2. Contours of the electric field component having the proper polarization for ion absorption for $m = -1$.

RF POWER ABSORPTION SIMULATION

The RF power absorption by the plasma for a given antenna current determines the plasma loading resistance, a figure of merit for the antenna design. In a lumped circuit model, the resistance for each antenna segment can be defined as twice the power emitted by that segment divided by the square of the current in that segment. In order to efficiently couple RF power to the plasma, the loading resistance for the entire antenna must be substantially larger than the vacuum loading resistance, which is due to the finite resistance of the entire antenna driving circuit.

For a good antenna design, a reasonably accurate model of the RF absorption can be based using only the dingle dominant mode. For more accurate calculations, several m modes are used and the system (5) is solved independently for each m .

Figure 2 shows contour plots of the RF electric field amplitudes and absorbed power for the $m = -1$ mode propagating from the antenna up to a region where w is equal to the ion gyro-frequency. The $m = -1$ mode penetrates to the axis with the correct polarization to accelerate ions in the direction perpendicular to the static magnetic field (a good antenna design for the ICRF section will excite primarily the $m = -1$ mode with a high loading resistance)

The numerical algorithm conserves energy in the system globally. If sufficient resolution is used in a cold plasma model, then the traditional Poynting's theorem,

$$\int_V \frac{1}{2} \text{Re}[\mathbf{E} \cdot (\mathbf{j}_p + \mathbf{j}_{ANT})^*] dV + \oint_{\partial V} \text{Re}(\mathbf{S} \cdot \mathbf{n}) d(\partial V) = 0 \quad (11)$$

can be considered, and convergence can be determined by the presence of positive definite plasma absorption at every location in the system. Here $\mathbf{S} = (\mathbf{E} \times \mathbf{B}^*) / (2\mu)$ is the complex Poynting vector and \mathbf{n} is the unit vector normal to the integration surface.

The numerical simulation of the ICRF-plasma interaction was conducted for a reference density profile and particle flux as measured in the VASIMR

experiment using curve fits from a Langmuir triple probe and from a Mach probe. Fixed electron and ion temperatures of 4 and 2 eV, respectively, were chosen to reduce the number of the variable parameters.

The new EMIR model allows the simulation of wave-plasma interactions with greater physical accuracy than in the previous cold plasma model. As shown in Figures 3 and 4, the power density distribution vs. longitudinal coordinate (and therefore vs. axial magnetic field) features peak shifted downstream from the cold plasma ion cyclotron resonance due to the Doppler effect.

The Figure 5 demonstrates the effect of the plasma flow velocity on the Doppler shift. Numerical simulations show that a higher flow velocity moves the location of the power absorption downstream from the cold resonance and increases the ratio of ion to electron absorbed power for most values of the RF frequency.

An important goal for of the ICRF antenna design is to achieve high RF antenna loading. Since the absorbed RF power is proportional to the plasma

loading as $P_{ANT} = \frac{1}{2} R_p I_{ANT}^2$, the EMIR simulation

allows calculating the loading from the absorbed power for any given antenna current. The plasma loading R_p is being compared with the circuit loading R_c to analyze the fraction of the ICRF power going into plasma.

The present experiment and simulation results indicate that a measurable amount of RF power, up to 40%, reaches the plasma. Simulations suggest that more than 50% of the power coupled to the plasma goes to ions rather than electrons when the ion gyrofrequency is tuned near the antenna. This level of power coupling provides measurable changes to the ion energy distribution, on the order of 25 to 50 eV added per ion Figure 6 demonstrates good agreement of the plasma loading calculated by EMIR for Helium and Argon plasma with experimental measurements. The input parameter of the ICRF frequency was varied to find the optimal ICRF regime. The EMIR code was run both with the cold the plasma model and with the new kinetic reduced order model, for comparison.

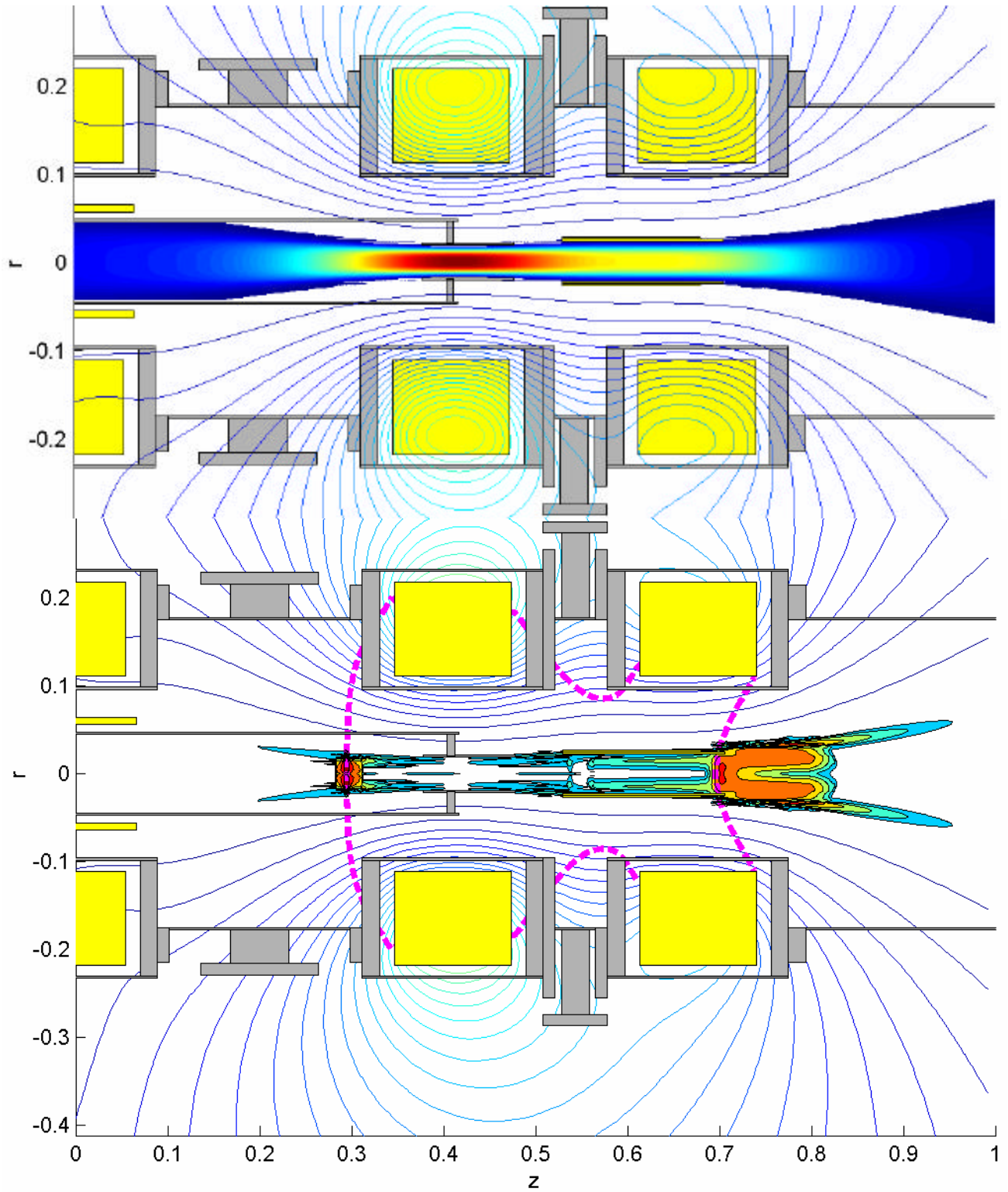


Figure 3. Plasma density n_i (top) and RF Power density $E \cdot (\hat{S} E)^*$ contours for the VASIMR magnetic configuration. Dashed line shows the area of the cold ICRF resonance, i. e. $B_0 = \omega m_i / q_i$.

CONCLUSIONS

An effective ion cyclotron wave coupling to the plasma has been in the VASIMR experiment. The baseline plasma parameters considered in the latest ICRF antenna design give a plasma loading with $R_p \sim R_c$, that is about half of the RF transmitter power gets absorbed by the plasma, with more than half directly coupled to the ions. Future design improvements are directed to increase the overall VASIMR efficiency by minimizing the RF circuit losses, increasing the plasma flux from the helicon source and optimizing the magnetic geometry.

The EMIR simulation of the RF wave propagation in the VASIMR plasma allows to design the ICRF

antenna with improved efficiency, as well as to optimize the magnetic field profile.

The recent developments in the EMIR code resulted in a code performance improvement that will enable further refinement in the physics of the model without sacrificing the fast turnaround of simulation results that is required by the present design effort to support the VASIMR experiment.

ACKNOWLEDGMENTS

This research was supported by NASA code M and the NASA Johnson Space Center.

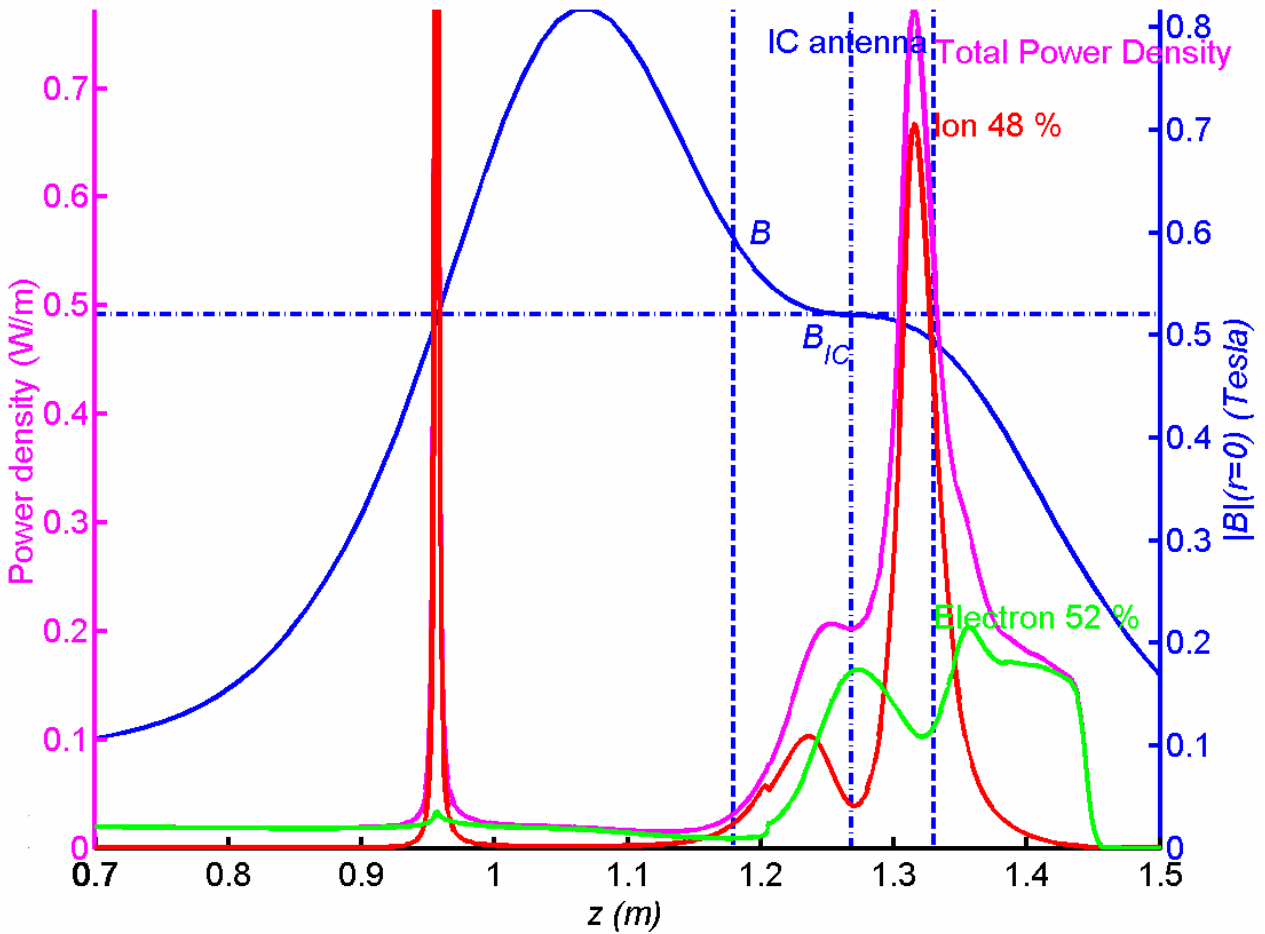


Figure 4. Magnetic field configuration for the VASIMR experiment with the ICRF power absorption calculated by the EMIR code. Vertical lines indicate the ICRF antenna boundaries. The absorbed power density has two peaks. The first peak indicates the IC resonance upstream the plasma flow. Due to the Doppler shift, most of the total power gets absorbed by the plasma downstream from the cold ICRF resonance, marked in the picture by the vertical dashed line B_{IC} .

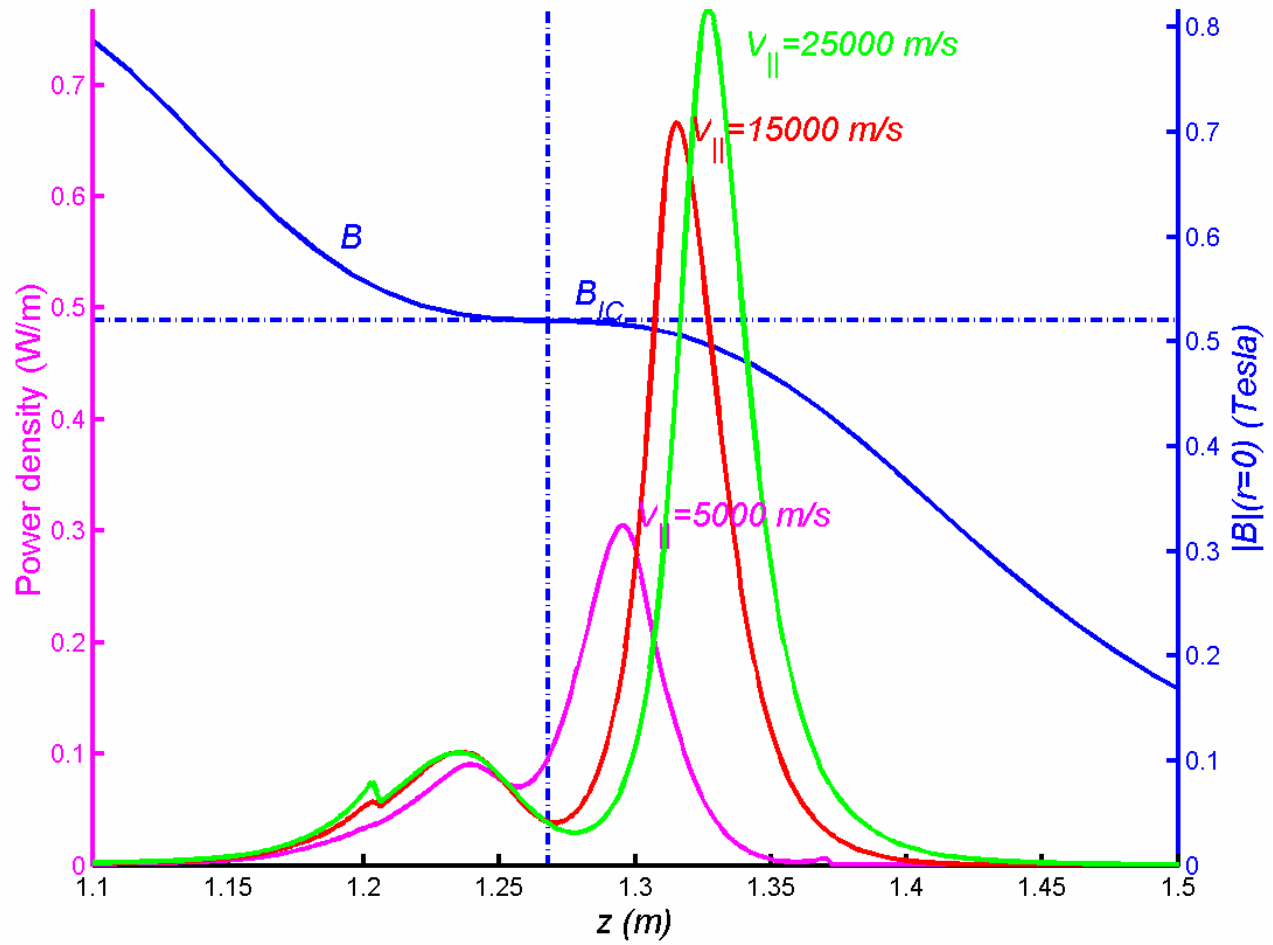


Figure 5. Magnetic field configuration for the VASIMR experiment with the ICRF power density absorbed by the ions shown for different values of the plasma flow velocity $V_{||}$.

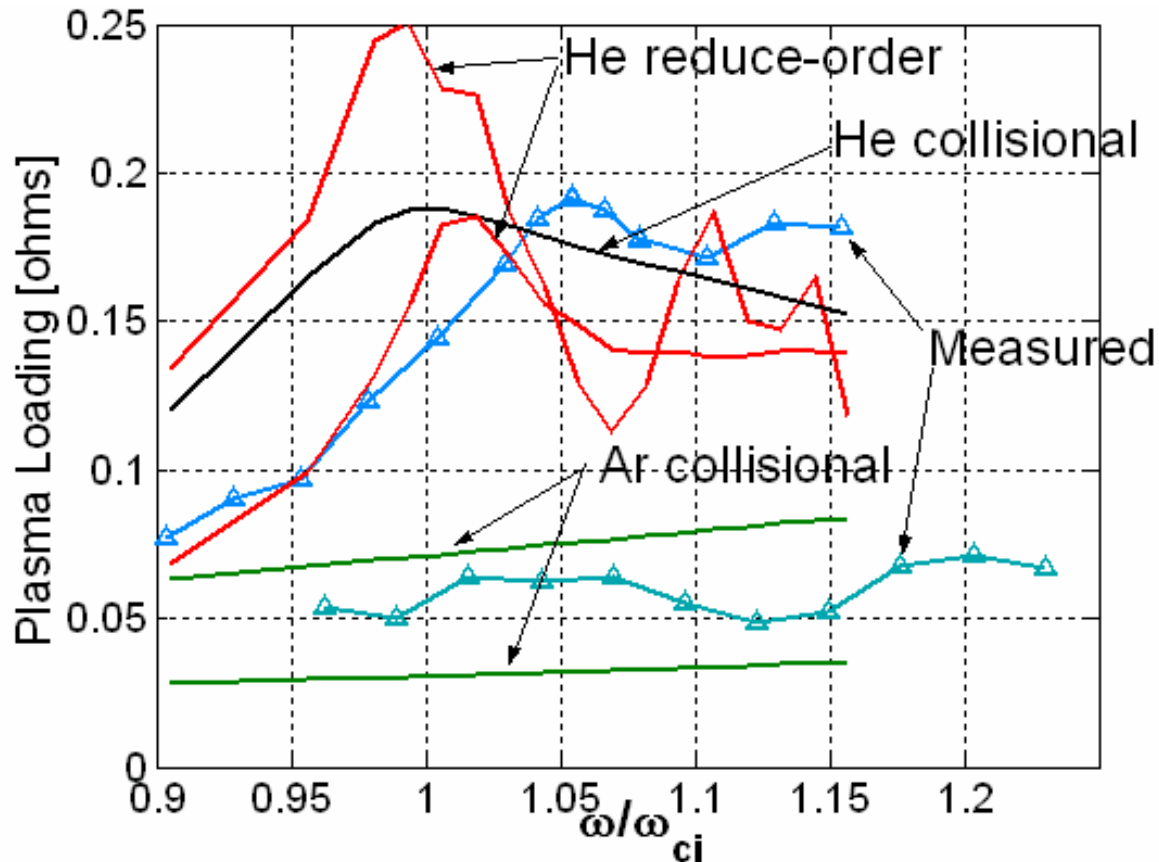


Figure 6. Comparison of simulation results with experimental data on the RF loading for VASIMR discharges with Helium and Argon plasma. All calculated curves use a 4 eV electron temperature. The two reduced-order curves represent the range of results by varying plasma flow profiles and choosing different propagating roots. The two calculated argon curves represent a large range in the neutral collision rate ($4 - 24 \cdot 10^6 \text{ s}^{-1}$), with the lower loading corresponding to the lower rate. The helium collisional curve is a representative case, since there is not a strong sensitivity to parameters.

REFERENCES

1. Chang Díaz F. R., "The VASIMR engine", *Scientific American*, **283** (2000) 72-79.
2. Chang Díaz F. R., "An Overview of the VASIMR Engine: High Power Space Propulsion with RF Plasma Generation and Heating", *Proceedings of 14th Topical Conference on Radio Frequency Power in Plasmas*, May 7-9, 2001, Oxnard, CA, (2001).
3. Jaeger E. F., Batchelor D. B., Weitzner H., Whealton J.H. "ICRF Wave Propagation And Absorption in Tokamak And Mirror Magnetic Fields - A Full-wave Calculation", *Computer Physics Com.*, **40** (1986) 33 – 64.
4. Stix T. H. "Waves in Plasmas", American Institute of Physics, New York, (1992).
5. Colestock P., Kashuba R. J. "The theory of mode conversion and wave damping near the ion cyclotron frequency", *Nuclear Fusion*, **23** (1983).
6. Carter M. D., Baity F. W., Barber G. C., Goulding R. H., Mori Y., Sparks D. O., White K. F., Jaeger E. F., Chang Díaz F. R., Squire J. P. "Comparing Experiments with Modeling for Light Ion Helicon Plasma Sources", *Physics of Plasmas*, **9** (2002) 5097 – 5110.
7. Ilin, A. V., Chang Díaz, F. R., Squire, J. P., Breizman, B. N., and Carter, M. D., "Particle Simulations of Plasma Heating in VASIMR", *Proceedings of 36th AIAA/ASME/SAE/ASEE Joint Propulsion Conference* July 17-19, 2000, Huntsville, AL, AIAA 2000-3753 (2000) 10.